Wireless Network Coding with Intelligent Reflecting Surfaces

Thesis by

Amanat Kafizov

In Partial Fulfillment of the Requirements

For the Degree of

Masters of Science

King Abdullah University of Science and Technology

Thuwal, Kingdom of Saudi Arabia

April, 2021

EXAMINATION COMMITTEE PAGE

The thesis of Amanat Kafizov is approved by the examination committee

Committee Chairperson: Prof. Mohamed-Slim Alouini
Committee Members: Prof. Basem Shihada, Prof. Meriem Laleg and Dr. Abla Kammoun

ABSTRACT

Wireless Network Coding with Intelligent Reflecting Surfaces

Amanat Kafizov

Conventional wireless techniques are becoming inadequate for beyond fifth-generation (5G) networks due to latency and bandwidth considerations. To increase the wireless network throughput and improve wireless communication systems' error performance, we propose physical layer network coding (PNC) in an Intelligent Reflecting Surface (IRS)-assisted environment. We consider an IRS-aided butterfly network, where we propose an algorithm for obtaining the optimal IRS phases. Also, analytic expressions for the bit error rate (BER) are derived. The numerical results demonstrate that the scheme proposed in this thesis significantly enhances the BER performance. The proposed scheme is compared to traditional network coding without IRS. For instance, at a target BER of 10^{-3}, 28 dB and 0.75 dB signal to noise ratio (SNR) gains are achieved at the relay and destination node of the 32-element IRS-assisted butterfly network model.

ACKNOWLEDGEMENTS

I would like to acknowledge every person who played a vital role in my academic achievements. First of all, my family, who supported me throughout my master's journey at KAUST. Without them, I could never stand where I am today. Secondly, my graduate study supervisor Prof. Mohamed-Slim Alouini, who accepted my Ms/Ph.D. application to KAUST, provided useful advice whenever I needed it, and guided me throughout my academic life at KAUST. Also, I want to express thankfulness to my research supervisor Dr. Ahmed Elzanaty, a post-doctoral fellow at KAUST. He provided incredible guidance and was ready to help whenever I had questions about my research.

I also would like to give special thanks to Dr. Abla Kammoun, Prof. Meriem Laleg, Prof. Basem Shihada, and Prof. Ahmed Sultan Salem, and members of the Communication Theory Lab for their help both in research and courses.

TABLE OF CONTENTS

LIST OF ABBREVIATIONS

5G	fifth-generation
BER	bit error rate
BPSK	binary phase shift keying
CCP	concave convex procedure
CSI	channel state information
DC	difference-of-convex functions
EM	electromagnetic
IoT	Internet of Things
IRS	Intelligent Reflecting Surface
LLR	log likelihood ratio
mm-Wave	millimeter wave
MMSE	minimum mean square error
mMTC	massive machine type communication
MSE	mean-squared error
NC	network coding
NNC	network-layer network coding
OAC	over-air-computation
PNC	physical layer network coding
QPSK	quadrature phase shift keying
SDP	semi-definite program
SDR	semi-definite relaxation
SNR	signal to noise ratio

LIST OF FIGURES

Chapter 1

Introduction

In the modern world, wireless networks are becoming more ubiquitous because they connect not only people but also their devices. It is predicted that in the near future, billions of low-cost Internet of Things (IoT) devices, which can be used for sensing and communication, will have connectivity to wireless networks; thus, our daily life operations can be operated automatically [1, 2]. All this results in the inevitable increase of the density of the wireless networks, which in turn leads to the reduced capacity available per node.

Another critical problem is the need to collect and process the data from these vast number of IoT devices in beyond fifth-generation (5G) wireless networks. Today, a high data rate is required in order to perform ultra-fast wireless data aggregation in on-device federated machine learning and massive machine type communication (mMTC), which are the principal use cases of beyond 5G wireless networks. However, conventional wireless communication techniques become infeasible because they, in general, account for excessive network latency and low spectrum utilization efficiency [1, 3].

All this suggests that it is time for exploring new technologies in wireless networking. Therefore, in this thesis, network coding (NC) with Intelligent Reflecting Surface (IRS) is proposed to increase throughput and enhance the bit error rate (BER) performance of the wireless network.

1.1 Network Coding

Network coding is considered a promising solution to enhance the throughput of wireless networks. It relies on a router or relay's ability to execute more complex operations in addition to just forwarding [1,4,5]. NC can be performed at the network layer or the physical layer. According to network-layer network coding (NNC), the relay computes network coded form from the data it received and, then, forwards it further. The NNC model assumes that the data from the source nodes arrive at the relay over discrete links, which is necessary to avoid interference. In a wireless medium, it can be achieved by applying time-division multiple access to allocate orthogonal channels for the links. The relay can then decode the data on these links separately before computing the network-coded form. However, according to information theory, the greater capacity can often be achieved when the source nodes send the data simultaneously at the same time in non-orthogonal channels [1].

Physical layer network coding (PNC) increases the throughput of the network by exploiting the physical broadcast nature of wireless links, which generally causes deleterious interference [1, 4–7]. In particular, instead of mitigating the interference, PNC takes advantage of it to improve the throughput performance. In PNC, source nodes transmit simultaneously in the same frequency channel and in the same time-slot. Hence, the relay receives a superposition of electromagnetic (EM) waves of the wireless signals because, at the wireless communication's physical layer, the signals are sent through EM waves [1,6]. This approach will be described more rigorously in the later chapters.

Yet, higher bandwidth is required to support PNC with higher data rates, which necessitates a move toward the millimeter wave (mm-Wave) band. mm-Wave has a huge bandwidth, i.e. 30-300 GHz, to support Gigabit-per-second data transmission in wireless applications such as virtual reality, online gaming, federated learning, etc. Nevertheless, mm-Wave communication suffers from high path loss and is suscepti-

ble to blockages. These limitations suggest future sustainable networks, where the propagation channel itself can be controlled [8–10].

1.2 Intelligent Reflecting Surface

In this regard, so-called IRSs have been demonstrated to overcome some of the issues associated with mm-Waves since it can smartly reconfigure the wireless radio/channel propagation environment [11, 12]. An IRS is a flat surface that comprises many small passive elements. Each element can independently introduce controllable phase changes to the incident signals [13]. Smartly tuning the phases of IRS enables the reconfiguration of the signal wireless channels between transmitting and receiving nodes. Hence, the desired realization of the channels can be achieved, meaning that the interference issue and the wireless channel fading impairment can be tackled fundamentally. Integrated electronics can be used to control IRS [11, 13, 14].

There are also practical benefits of implementing IRS. First, unlike traditional relays, IRSs do not need a dedicated energy source or consume any transmit power; thus, much lower hardware and energy cost is needed to implement and manage them compared to traditional relays. Moreover, IRS does not amplify the noise, does not have a self-interference issue, and operates in full-duplex mode, while traditional half-duplex and full-duplex relays suffer from low spectral efficiency and self-interference issue, respectively. Furthermore, an IRS is of conformal geometry, low profile, and light weight; therefore, it can be easily mounted into ceilings, walls, and building facades [13, 15].

Due to the above benefits, IRSs can enhance wireless communication performance in terms of coverage, energy efficiency, electromagnetic radiation reduction, and wireless localization accuracy [16–20]. Also, IRSs can improve the BER performance of over-air-computation (OAC) techniques, which leverage the superposition property in multiple-access channel from sources to a relay [14, 21, 22]. It can achieved by

intelligently tuning the IRS phase profile, thereby significantly boosting the received signal power at the desired receiver. In a sense, PNC is a kind of OAC as it is based on the linear or nonlinear aggregation of signals by the wireless medium; yet it has remained unstudied in the presence of IRSs.

1.3 Main Contributions

This thesis proposes a PNC scheme in an IRS-assisted environment to enhance the performance of wireless communication systems, especially in unfavorable channel conditions for mm-Wave communication. As a proof of concept, we focus on the butterfly network, usually adopted as the basic setting in the framework of network coding [6, 23]. In the butterfly network, the relay computes network-coded packets directly from the received signal. To improve BER performance, we optimize the IRS phase profile and beamforming matrix at the relay. Notwithstanding that the optimization problem has non-convex constraints, we convexify it and propose an efficient optimization algorithm based on matrix lifting. Then, we derive the analytic expressions of BER of IRS-aided butterfly network to judge error performance. Simulation results verify our finding of 2 dB gain due to IRS and PNC.

1.4 Outline and Notation

The rest of this thesis is organized as follows. The system model is described in Chapter 2. In Chapter 3, the optimization problem is formulated, and the optimization algorithm is described. Chapter 4 illustrates the optimal detection and error performance. Chapter 5 presents numerical results. Thesis is concluded in Chapter 6.

For notation, the probability of an event is denoted by $\mathbb{P}\{\cdot\}$, and the expectation of a random variable is denoted by $\mathbb{E}[\cdot]$. Capital bold letters, e.g., $\mathbf{C}$, and small bold letters, e.g., $\mathbf{c}$, denote matrices and vectors, respectively. A diagonal matrix

with diagonal elements from vector $\mathbf{c}$ is denoted by $\text{diag}(\mathbf{c})$, while $\text{tr}\,(\cdot)$ denotes the matrix trace. The transpose and Hermitian of vectors or matrices are denoted as $(\cdot)^T$ and $(\cdot)^H$. The notations $\mathbf{c}_{(l)}$ and $\mathbf{c}_l$ mean the l^{th} row and column of a matrix $\mathbf{C}$, respectively. The (k,l)th element of matrix $\mathbf{C}$ is denoted as c_{kl}. The notation $\Re(z)$ denotes the real part of complex number z. The notation $||\mathbf{c}||$ represents the ℓ_2-norm of a vector $\mathbf{c}$.

Chapter 2

System Model

This thesis considers the IRS-aided butterfly network as shown in Fig. 2.1, where sources S_1 and S_2 want to deliver their messages to destinations D_1 and D_2. For simplicity, we assume each destination and source node have a single antenna to receive and transmit, respectively, whereas the relay node has $N_r = 2$ antennas to transmit/receive. To enhance communication performance from $N_s = 2$ sources to relay, we propose deploying an IRS that comprises M reflecting elements, as in Fig. 2.1.

There are two stages in PNC. In the first stage, S_1 and S_2 broadcast their data to the relay and to destinations D_1 and D_2, respectively. Signals from S_1 and S_2 are assumed to arrive at the relay with symbol-level synchronization [1]. Let P and s_i be the transmit power and the transmitted symbol of source i, respectively. Hence, the signal transmitted by source i is $x_i = \alpha_i s_i$, where $\alpha_i = \sqrt{P/\sigma_{s,i}^2}$. The power of s_i is $\mathbb{E}\left[|s_i|^2\right] = \sigma_{s,i}^2$. We assume binary phase shift keying (BPSK) modulation at source nodes, but this also can be extended to quadrature phase shift keying (QPSK). The noise at the relay's jth antenna is assumed to be complex Gaussian with zero mean and σ^2 variance, i.e., $n_j \sim \mathcal{CN}(0, \sigma^2)$. The Rayleigh fading channels are assumed between IRS and relay, between sources and IRS, between sources and relay, between S_1 and D_1, and between relay and D_1 as $\mathbf{H^{ir}} \in \mathbb{C}^{N_r \times M}$, $\mathbf{H^{ui}} \in \mathbb{C}^{M \times N_s}$, $\mathbf{H^{ur}} \in \mathbb{C}^{N_r \times N_s}$, $h_{D_1}^{S_1} \in \mathbb{C}^{1\times 1}$ and $\mathbf{h}_{D_1}^{r} \in \mathbb{C}^{1\times N_r}$, respectively. The signal received at the relay node can

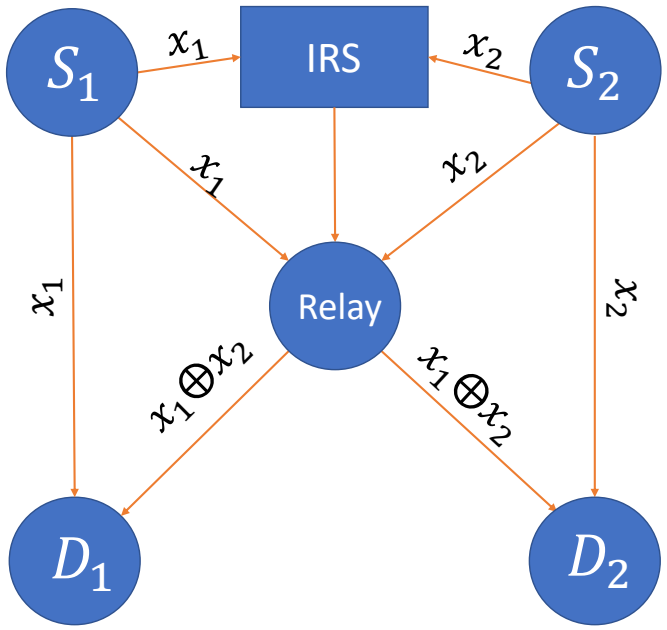

Figure 2.1: IRS-Aided Butterfly Network.

be written in a matrix form as

$$\mathbf{r} = \left(\mathbf{H}^{\mathbf{ir}}\mathbf{\Theta}\mathbf{H}^{\mathbf{ui}} + \mathbf{H}^{\mathbf{ur}}\right)\mathbf{x} + \mathbf{n} \triangleq \mathbf{H}\mathbf{x} + \mathbf{n}, \tag{2.1}$$

where $\mathbf{\Theta} = \text{diag}\,(\mathbf{v})$ is the diagonal phase shift matrix of IRS with $\mathbf{v} = \left[e^{j\theta_1}, \ldots, e^{j\theta_M}\right]^T$ and $\theta_m \in [0, 2\pi]$, $\mathbf{x} = [x_1, x_2]^T$ is the signal vector, and $\mathbf{n} = [n_1, n_2, \ldots, n_{N_\text{r}}]^T$ is the noise vector.

In the second stage, the relay computes an estimate of the XOR of the signals from S_1 and S_2. Here, the XORed version is considered as a network-coded form created out of the signals from source nodes. After that, the relay broadcasts the estimated network-coded signal to D_1 and D_2. Thus, D_1 receives a signal from S_1 and a network-coded signal from the relay, and can calculate the signal from S_2 by XORing the received signals. D_2 can perform an equivalent process.

In traditional network-layer network coding (NNC) rather than PNC, the relay computes the estimates of x_1 and x_2 before creating a network-coded form $x_\oplus \triangleq$

$x_1 \oplus x_2$. However, such schemes are suboptimal since they do not consider that only $x_\oplus$ is needed at the relay rather than individual signals x_1 and x_2 [1,6]. For example, if matrix $\mathbf{H}$ does not have a full rank, the relay will not be able to recover x_1 and x_2 individually from $\mathbf{r}$. Hence, NC scheme has a zero multiple access rate of $x_\oplus$.

Therefore, we propose the PNC approach where the relay computes an estimate of $x_\oplus$ without decoding x_1 and x_2 individually. In fact, it is more useful to get the estimate of $x_\oplus$ from x_1+x_2 and x_1-x_2, which are able to be calculated instantly from $\mathbf{r}$ via matrix multiplication. Hence, the relay can get $x_\oplus$ almost at full rate [6, 24].

Based on this observation, the received signal in (2.1) is rewritten as

$$\mathbf{r} = \left(\mathbf{H}\mathbf{D}^{-1}\right)(\mathbf{D}\mathbf{x}) + \mathbf{n} = \widetilde{\mathbf{H}}\widetilde{\mathbf{x}} + \mathbf{n}, \tag{2.2}$$

where

$$\mathbf{D} = 2\mathbf{D}^{-1} = \begin{bmatrix} 1 & 1 \\ 1 & -1 \end{bmatrix} \tag{2.3}$$

is the sum-difference matrix, and $\widetilde{\mathbf{x}}$ is

$$\widetilde{\mathbf{x}} = \begin{bmatrix} \widetilde{x}_1 \\ \widetilde{x}_2 \end{bmatrix} \triangleq \mathbf{D}\,\mathbf{x} = \begin{bmatrix} x_1 + x_2 \\ x_1 - x_2 \end{bmatrix}. \tag{2.4}$$

The vector $\widetilde{\mathbf{x}}$ can be estimated from $\mathbf{r}$ using a linear operator as

$$\mathbf{y} = \mathbf{G}\mathbf{r}, \tag{2.5}$$

where $\mathbf{G} \in \mathbb{C}^{N_\mathrm{s} \times N_\mathrm{r}}$ is the beamforming matrix at the relay, designed in Chapter 3. We consider that the relay can estimate the channel state information (CSI).

Chapter 3

Optimization

3.1 Formulation of the Optimization Problem

In this chapter, our objective is to design the optimal linear operator, i.e., the beamforming matrix $\mathbf{G}$ and the IRS phase profile $\boldsymbol{\Theta}$ to minimize the mean-squared error (MSE) for the recovery of $\widetilde{\mathbf{x}}$. In this regard, the optimization problem is formulated as

$$\underset{\boldsymbol{\Theta},\mathbf{G}}{\text{minimize}} \quad \mathsf{MSE} \triangleq \mathbb{E}\left[\|\mathbf{y}(\boldsymbol{\Theta},\mathbf{G}) - \widetilde{\mathbf{x}}\|^2\right] \tag{3.1a}$$

$$\text{subject to} \quad 0 \leq \theta_m \leq 2\pi,\ m \in \{1,2,\ldots,M\}. \tag{3.1b}$$

The MSE between target parameter $\widetilde{\mathbf{x}}$ and its estimate $\mathbf{y}$ can be computed as

$$\begin{aligned}\mathsf{MSE} &= \mathrm{tr}\left(\mathbb{E}\{(\mathbf{G}\mathbf{r} - \widetilde{\mathbf{x}})\left(\mathbf{r}^H\mathbf{G}^H - \widetilde{\mathbf{x}}^H\right)\}\right)\\ &= \mathrm{tr}\left(\mathbf{G}\mathbb{E}\{\mathbf{r}\mathbf{r}^H\}\mathbf{G}^H - 2\Re\{\mathbf{G}\mathbb{E}\{\mathbf{r}\widetilde{\mathbf{x}}^H\}\} + \mathbb{E}\{\widetilde{\mathbf{x}}\widetilde{\mathbf{x}}^H\}\right)\\ &= \mathrm{tr}\left(\mathbf{G}(P\mathbf{H}\mathbf{H}^H + \sigma^2\mathbf{I})\mathbf{G}^H - 2\Re\{\mathbf{G}P\mathbf{H}\mathbf{D}^H\} + 2P\mathbf{I}\right).\end{aligned} \tag{3.2}$$

The joint optimization over the beamforming matrix and IRS profile in (3.1) is challenging. In Chapter 3, we provide an efficient algorithm for the optimization problem.

3.2 Optimization Algorithm

In this thesis, an iterative algorithm is proposed that alternately optimizes the IRS phases while fixing the beamforming matrix in (3.1). In particular, for a fixed $\boldsymbol{\Theta}$ in (3.1), the optimization problem is a quadratic unconstrained problem, where MSE depends only on the matrix $\mathbf{G}$. Taking derivative of MSE with respect to $\mathbf{G}$

$$\frac{d\mathsf{MSE}}{d\mathbf{G}} = 2\mathbf{G}(P\mathbf{H}\mathbf{H}^H + \sigma^2\mathbf{I}) - 2P\mathbf{D}\mathbf{H}^H = 0, \tag{3.3}$$

the closed-form solution is

$$\mathbf{G} = P\mathbf{D}\mathbf{H}^H \left(P\mathbf{H}\mathbf{H}^H + \sigma^2\mathbf{I}\right)^{-1}, \tag{3.4}$$

which is the minimum mean square error (MMSE) estimator for $\mathbf{G}$. To optimize the phases of IRS for fixed $\mathbf{G}$, we propose the matrix lifting technique [25]. First, the objective function should be written in terms of $\mathbf{v}$, i.e., MSE can be written as

$$\begin{aligned}\mathsf{MSE} \triangleq P\sum_{i'=1}^{N_\mathrm{s}}\sum_{j\prime=1}^{N_\mathrm{r}}\left(\sum_{j=1}^{N_\mathrm{r}}\mathbf{g}_j^H\mathbf{g}_{j'}\left(b^{ji'}\right)^H\right)b^{j'i'} + 2PN_\mathrm{s} \\ - 2P\Re\left(\sum_{i=1}^{N_\mathrm{s}}\sum_{j=1}^{N_\mathrm{r}} b^{ji}\left(g_{1j} + (-1)^{i+1}g_{2j}\right)\right) + \sum_{i=1}^{N_\mathrm{s}}{\sigma_i}^2,\end{aligned} \tag{3.5}$$

where $b^{ji} = \boldsymbol{\phi}^{ji}\mathbf{v} + h_{ji}^{ur}$ and $\boldsymbol{\phi}^{ji} = \mathbf{h}_{(j)}^{\mathbf{ir}}\,\mathrm{diag}(\mathbf{h}_i^{\mathbf{ui}})$.

By substituting (3.4) in (3.5), we can write the optimization problem (3.1) for a fixed $\mathbf{G}$ as:

$$\underset{\mathbf{v}}{\text{minimize}} \quad \mathsf{MSE} \tag{3.6a}$$

$$\text{subject to} \quad |\mathbf{v}(m)|^2 = 1,\ m \in \{1, 2, \ldots, M\}. \tag{3.6b}$$

The unit modulus constraint, (3.6b), induces non-convexity in optimization problem

Algorithm 1 Algorithm of optimizing $\mathbf{V}$ for fixed $\mathbf{G}$

1: **Initialize** $\mathbf{V}_{\text{iter}}$ as in (3.7) with an arbitrary vector $\mathbf{v}$ that satisfies (3.6b) and set iter $= 1$
2: **repeat**
3: **Step 1:** Set $\mathbf{V}' := \mathbf{V}_{\text{iter}}$
4: **Step 2:** Solve convex problem (3.14), whose output is $\mathbf{V}$.
5: **Step 3:** Update $\mathbf{V}_{\text{iter}} := \mathbf{V}$
6: **Step 4:** Set iter $=$ iter $+ 1$
7: **until** $||\mathbf{V}_{\text{iter}} - \mathbf{V}'|\,|_F^2 \leq \delta_1$ or iter $> \text{Iter}_{\max}$
8: $\mathbf{V} := \mathbf{V}_{\text{iter}}$
9: **Output** $\mathbf{V}$

(3.6). In this regard, we apply a matrix lifting technique [25]. Now, the problem is tackled with the help of matrix $\mathbf{V}$, where

$$\mathbf{V} = \begin{bmatrix} \mathbf{v} \\ 1 \end{bmatrix} \begin{bmatrix} \mathbf{v}^H & 1 \end{bmatrix} = \begin{bmatrix} \mathbf{v}\mathbf{v}^H & \mathbf{v} \\ \mathbf{v}^H & 1 \end{bmatrix}. \tag{3.7}$$

For $\mathbf{V}$, we have the following constraints: $\text{rank}\,(\mathbf{V}) = 1$, $\mathbf{V} \geq 0$, and $\mathbf{V}(k,k) = 1$, $\forall k \in \{1, \ldots, M+1\}$. Let us rewrite (3.5) in terms of $\mathbf{V}$ and remove all the terms that do not depend on $\mathbf{v}$:

$$\begin{aligned} \mathsf{MSE} \propto & \sum_{i'=1}^{N_\text{s}} \sum_{j'=1}^{N_\text{r}} \sum_{j=1}^{N_\text{r}} \text{tr} \left(\mathbf{g}_j^H \mathbf{g}_{j'} \begin{bmatrix} \boldsymbol{\phi}^{ji'H} \boldsymbol{\phi}^{j'i'} & \boldsymbol{\phi}^{ji'H} h_{j'i'}^{ur} \\ h_{ji'}^{*ur} \boldsymbol{\phi}^{j'i'} & 0 \end{bmatrix} \mathbf{V} \right) \\ & - \sum_{i=1}^{N_\text{s}} \sum_{j=1}^{N_\text{r}} \text{tr} \left(\begin{bmatrix} 0 & \left(g_{1j}^* + (-1)^{i+1} g_{2j}^*\right) \boldsymbol{\phi}^{jiH} \\ 0 & 0 \end{bmatrix} \mathbf{V} \right) \\ & - \sum_{i=1}^{N_\text{s}} \sum_{j=1}^{N_\text{r}} \text{tr} \left(\begin{bmatrix} 0 & 0 \\ \left(g_{1j} + (-1)^{i+1} g_{2j}\right) \boldsymbol{\phi}^{ji} & 0 \end{bmatrix} \mathbf{V} \right) \\ = & \, \text{tr}\,(\mathbf{A}\mathbf{V}), \end{aligned} \tag{3.8}$$

where $\mathbf{A}$ is a matrix representing the summation of all the matrices inside the trace

functions in (3.8), i.e.,

$$\begin{aligned}\mathbf{A} = &\sum_{i'=1}^{N_{\mathrm{s}}}\sum_{j\prime=1}^{N_{\mathrm{r}}}\sum_{j=1}^{N_{\mathrm{r}}}\mathbf{g}_j^H\mathbf{g}_{j'}\begin{bmatrix}\boldsymbol{\phi}^{ji'H}\boldsymbol{\phi}^{j'i'} & \boldsymbol{\phi}^{ji'H}h_{j'i'}^{ur}\\ h_{ji'}^{*ur}\boldsymbol{\phi}^{j'i'} & 0\end{bmatrix}\\ &-\sum_{i=1}^{N_{\mathrm{s}}}\sum_{j=1}^{N_{\mathrm{r}}}\begin{bmatrix}0 & \left(g_{1j}^* + (-1)^{i+1}g_{2j}^*\right)\boldsymbol{\phi}^{jiH}\\ 0 & 0\end{bmatrix}\\ &-\sum_{i=1}^{N_{\mathrm{s}}}\sum_{j=1}^{N_{\mathrm{r}}}\begin{bmatrix}0 & 0\\ \left(g_{1j} + (-1)^{i+1}g_{2j}\right)\boldsymbol{\phi}^{ji} & 0\end{bmatrix}.\end{aligned} \tag{3.9}$$

So, we have the following optimization problem:

$$\underset{\mathbf{V}\geq 0}{\text{minimize}} \quad \mathrm{tr}\left(\mathbf{AV}\right) \tag{3.10a}$$

$$\text{subject to} \quad \mathbf{V}(k,k) = 1,\ k \in \{1,2,\ldots,M+1\} \tag{3.10b}$$

$$\mathrm{rank}\left(\mathbf{V}\right) = 1. \tag{3.10c}$$

The constraint $\mathrm{rank}\left(\mathbf{V}\right) = 1$ is non-convex, and the common way is to drop it using semi-definite relaxation (SDR) technique in order to address non-convexity in (3.10). Without rank-one constraint, (3.10) is convex semi-definite program (SDP) problem and can be solved by `cvx`. In general, the solution to the relaxed problem is not rank-one; therefore, an extra procedure named Gaussian randomization needs to be applied to get a sub-optimal solution. However, the complexity of such approach is significant since a sufficiently large number of randomizations is required to guarantee at least quasi-optimal solution [25, 26]. The constraint $\mathrm{rank}\left(\mathbf{V}\right) = 1$ is equivalent to

$$\mathrm{tr}\left(\mathbf{V}\right) - \beta_1\left(\mathbf{V}\right) = 0, \tag{3.11}$$

where $\beta_1\left(\cdot\right)$ denotes the largest singular value of the input matrix. Also, for $\mathbf{V} \geq 0$, i.e., semidefinite, the left side of (3.11) is 0 when $\mathrm{rank}\left(\mathbf{V}\right) = 1$ is satisfied; otherwise,

it is greater than zero. Now, instead of dropping the rank-one constraint in (3.10), the function (3.11) is added to the objective function as a penalty term, and the new optimization problem looks like

$$\underset{\mathbf{V}\geq 0}{\text{minimize}} \quad \left(\text{tr}\left(\mathbf{AV}\right) + \alpha\left(\text{tr}\left(\mathbf{V}\right) - \beta_1\left(\mathbf{V}\right)\right)\right) \tag{3.12a}$$

$$\text{subject to} \quad \mathbf{V}(k,k) = 1,\ k \in \{1, 2, \ldots, M+1\}, \tag{3.12b}$$

where $\alpha \geq 0$ is a fixed weight. Since $\beta_1\left(\mathbf{V}\right)$ and $\text{tr}\left(\mathbf{AV}\right) + \alpha\ \text{tr}\left(\mathbf{V}\right)$ are convex functions in $\mathbf{V}$, (3.12) is represented as a difference-of-convex functions (DC) problem. Concave convex procedure (CCP) can efficiently find a local optimal solution for DC problems [27]. Authors in [22] demonstrates that, in some cases, DC algorithm is able to find the exact one-rank solution when SDR with Gaussian randomization technique fails. In this regard, we linearize $-\alpha\,\beta_1(\mathbf{V})$, which induces non-convexity in (3.12), around a point $\mathbf{V} = \mathbf{V}'$ using the following upper bound [22]

$$-\alpha\,\beta_1\left(\mathbf{V}\right) \leq -\alpha\ \text{tr}\left(\mathbf{V}\mathbf{u_1}\left(\mathbf{V}'\right)\mathbf{u_1}\left(\mathbf{V}'\right)^H\right), \tag{3.13}$$

where $\mathbf{u_1}\left(\mathbf{V}'\right)$ outputs the eigenvector of $\mathbf{V}'$ corresponding to the largest eigenvalue, and how to set $\mathbf{V}'$ is shown in Alg. 1. The equality condition in (3.13) is satisfied when $\mathbf{V} = \mathbf{V}'$. We get the following convex optimization problem, whose optimal solution can be found using `cvx`:

$$\min_{\mathbf{V}\geq 0} \quad \text{tr}\left(\mathbf{AV}\right) + \alpha\left(\text{tr}\left(\mathbf{V}\right) - \text{tr}\left(\mathbf{V}\mathbf{u_1}\left(\mathbf{V}'\right)\mathbf{u_1}\left(\mathbf{V}'\right)^H\right)\right) \tag{3.14a}$$

$$\text{s.t.} \quad \mathbf{V}(k,k) = 1,\ k \in \{1, 2, \ldots, M+1\}. \tag{3.14b}$$

Appropriate choice of the penalty parameter α in (3.14) can be found via simple bisection method. It remains static throughout Alg. 1, and it is updated in Alg. 2. An algorithm that iteratively optimizes the phases of IRS and beamforming matrix

Algorithm 2 Iterative algorithm for MMSE optimization

1: **Initialize** $\mathbf{v}^1$ as an arbitrary vector that satisfies (3.6b) and set $k = 0$
2: **repeat**
3: **Step 1:** Set $k = k + 1$
4: **Step 2:** Update $\mathbf{G}^k$ using (3.4), where diagonal elements of phase matrix $\mathbf{\Theta}$ are the elements of vector $\mathbf{v}^k$
5: **Step 3:** Run Alg. 1, where $\mathbf{G} = \mathbf{G}^k$, and update $\mathbf{v}^{k+1}$ with the first M elements in $\mathbf{v}_{M+1}$
6: **until** $\left|\left|\mathbf{v}_{k+1} - \mathbf{v}^k\right|\right|^2 + \left|\left|\mathbf{G}_{k+1} - \mathbf{G}^k\right|\right|_F^2 < \delta_2$

$\mathbf{G}$ in an alternating manner is given in Alg. 2.

Chapter 4

Optimal Detector and Error Performance

For the scheme, MMSE estimator derived in (3.4) is the optimal one. However, multiplication of matrices $\mathbf{G}$ and $\widetilde{\mathbf{H}}$ results in a matrix, which is not always close to the identity matrix. For example, $\mathbf{G}\widetilde{\mathbf{H}} = \mathbf{I}$ is not accurate for the low SNR region if M is small or IRS is not used. The exact SNR regions will be given later in chapter 5. The optimal detector and error performance analysis below are derived assuming that the result of the multiplication of matrices $\mathbf{G}$ and $\widetilde{\mathbf{H}}$ is close to the identity matrix.

4.1 Optimal Detector

The likelihood estimator can be considered to estimate the network coding form, i.e., $x_{\oplus}$, from $\mathbf{y}$. In this regard, the log likelihood ratio (LLR) can be written, ignoring the noise dependencies in y_1 and y_2, as

$$\begin{aligned}
\mathcal{L}\left(x_{\oplus}|y_1y_2\right) &= \log\left(\frac{\mathbb{P}\{y_1y_2|x_{\oplus}=1\}}{\mathbb{P}\{y_1y_2|x_{\oplus}=-1\}}\right) \\
&= \log\left(\frac{\mathbb{P}\{y_1|\widetilde{x}_1=0\}\left[\mathbb{P}\{y_2|\widetilde{x}_2=2\}+\mathbb{P}\{y_2|\widetilde{x}_2=-2\}\right]}{\left[\mathbb{P}\{y_1|\widetilde{x}_1=2\}+\mathbb{P}\{y_1|\widetilde{x}_1=-2\}\right]\mathbb{P}\{y_2|\widetilde{x}_2=0\}}\right) \\
&= 2\left(\frac{1}{\sigma_1^2}-\frac{1}{\sigma_2^2}\right)+\log\left(\frac{\cosh\left(2y_2/\sigma_2^2\right)}{\cosh\left(2y_1/\sigma_1^2\right)}\right), \qquad (4.1)
\end{aligned}$$

where $\sigma_i^2 \triangleq \{\mathbf{G}\mathbf{G}^H\}_{i,i}\sigma^2$ is the noise variance on the ith stream after the linear operator.

Let us first define the estimation of $x_{\oplus}$ at the relay and D_1 as $\widehat{x}_{\oplus,\mathrm{r}}$ and $\widehat{x}_{\oplus,\mathrm{D}_1}$,

respectively. The corresponding decision rules are then:

$$\widehat{x}_{\oplus,\mathrm{r}} = \begin{cases} 1 & \text{when } \mathcal{L}\left(x_{\oplus}|y_1 y_2\right) \geq 0 \\ -1 & \text{when } \mathcal{L}\left(x_{\oplus}|y_1 y_2\right) < 0 \end{cases} \tag{4.2a}$$

$$\widehat{x}_{\oplus,\mathrm{D}_1} = \begin{cases} 1 & \text{when } \mathcal{L}^r_{\mathrm{D}_1}\left(\widehat{x}_{\oplus,\mathrm{r}}|y^r_{\mathrm{D}_1}\right) \geq 0 \\ -1 & \text{when } \mathcal{L}^r_{\mathrm{D}_1}\left(\widehat{x}_{\oplus,\mathrm{r}}|y^r_{\mathrm{D}_1}\right) < 0 \end{cases}, \tag{4.2b}$$

where $\mathcal{L}^r_{\mathrm{D}_1} = \log\left(\frac{\mathbb{P}\{y^r_{\mathrm{D}_1}|\widehat{x}_{\oplus,\mathrm{r}}=1\}}{\mathbb{P}\{y^r_{\mathrm{D}_1}|\widehat{x}_{\oplus,\mathrm{r}}=-1\}}\right) = 2y^r_{\mathrm{D}_1}/\sigma^2_{r,\mathrm{D}_1}$ is the likelihood detector, and $y^r_{\mathrm{D}_1}$ is the received signal at D_1 from relay. After the channel inversion, the variance of the noise at D_1 is $\sigma^2_{r,\mathrm{D}_1} = \sigma^2/\|\mathbf{h}^r_{\mathrm{D}_1}\|^2$. After that, the relay broadcasts $\widehat{x}_{\oplus,\mathrm{r}}$ to the destinations. D_1 receives $\widehat{x}_{\oplus,\mathrm{D}_1}$ and $\widehat{x}_1$, which is estimated similarly to $\widehat{x}_{\oplus,\mathrm{D}_1}$ with likelihood detector $\mathcal{L}^{\mathrm{S}_1}_{\mathrm{D}_1} = \log\left(\frac{\mathbb{P}\{y^{\mathrm{S}_1}_{\mathrm{D}_1}|x_1=1\}}{\mathbb{P}\{y^{\mathrm{S}_1}_{\mathrm{D}_1}|x_1=-1\}}\right) = 2y^{\mathrm{S}_1}_{\mathrm{D}_1}/\sigma^2_{\mathrm{S}_1,\mathrm{D}_1}$, received signal $y^{\mathrm{S}_1}_{\mathrm{D}_1}$, and noise variance after channel inversion $\sigma^2_{\mathrm{S}_1,\mathrm{D}_1} = \sigma^2/|h^{\mathrm{S}_1}_{\mathrm{D}_1}|^2$. Then, $\widehat{x}_2$ is obtained at D_1 by XORing $\widehat{x}_{\oplus,\mathrm{D}_1}$ and $\widehat{x}_1$. Similarly, D_2 receives $\widehat{x}_2$ and $\widehat{x}_{\oplus,\mathrm{D}_2}$, and obtains $\widehat{x}_1$ by XORing the two values.

4.2 BER Analysis

Before calculating instantaneous theoretical BER at D_1, i.e., $\mathbb{P}_{\mathrm{D}_1} \triangleq \mathbb{P}\left(\widehat{x}_2 \neq x_2\right)$, let us first find the instantaneous BERs separately for the links from sources to relay, from S_1 to D_1, and from relay to D_1.

Let us define the set $\mathbb{X} \triangleq \{-2, 2\}$, which contains all the values of $\widetilde{x}_2$ and $\widetilde{x}_1$ such that $x_{\oplus} = 1$ and $x_{\oplus} = -1$, respectively. To obtain $\widetilde{\mathbf{x}}$ at the relay from y_1 and y_2, we use the LLR in (4.1). To derive $\mathbb{P}^{\mathrm{r}}_{\oplus} \triangleq \mathbb{P}\left(\widehat{x}_{\oplus,\mathrm{r}} \neq x_{\oplus}\right)$ at the relay, we need to further rewrite (4.1) as

$$\mathcal{L}\left(x_{\oplus}|y_1 y_2\right) = \sum_{i=1}^{N_{\mathrm{s}}} (-1)^i \left[\log\left(\sum_{\widetilde{x}_i \in \mathbb{X}} e^{-\frac{(y_i - \widetilde{x}_i)^2}{2\sigma_i^2}}\right) + \frac{y_i^2}{2\sigma_i^2}\right]. \tag{4.3}$$

Now using the soft minimum approximation $\log\left(\sum_j \exp\left(-Z_j\right)\right) \approx -\min_j(Z_j)$ from [28], we can approximate the LLR in (4.3) as

$$\begin{aligned}\bar{\mathcal{L}}\left(x_{\oplus}|y_1y_2\right) &= \sum_{i=1}^{N_{\mathrm{s}}}(-1)^i\left[-\min_{\widetilde{x}_i\in\mathbb{X}}\left(\frac{(y_i-\widetilde{x}_i)^2}{2\sigma_i^2}\right)+\frac{y_i^2}{2\sigma_i^2}\right]\\ &= \sum_{i=1}^{N_{\mathrm{s}}}(-1)^{i+1}\min_{\widetilde{x}_i\in\mathbb{X}}\left(\frac{-2y_i\widetilde{x}_i+\widetilde{x}_i^2}{2\sigma_i^2}\right).\end{aligned} \tag{4.4}$$

Hence, instantaneous $\mathbb{P}^{\mathrm{r}}_{\oplus}$ can be approximated as

$$\begin{aligned}\mathbb{P}^{\mathrm{r}}_{\oplus} &\approx \mathbb{P}\{x_{\oplus}=1\}\mathbb{P}\{\bar{\mathcal{L}}<0|x_{\oplus}=1\}+\mathbb{P}\{x_{\oplus}=-1\}\mathbb{P}\{\bar{\mathcal{L}}\geq 0|x_{\oplus}=-1\}\\ &= \frac{1}{2}\left[Q\left(\frac{-2}{\sigma_2}\right)+Q\left(\frac{-2}{\sigma_1}\right)\right]Q\left(\frac{\sqrt{1+\frac{\sigma_2^2}{\sigma_1^2}}}{\sigma_2}\right)\\ &\quad + Q\!\left(\frac{2}{\sigma_2}\right)Q\!\left(\frac{-3+\frac{\sigma_2^2}{\sigma_1^2}}{\sigma_2\sqrt{1+\frac{\sigma_2^2}{\sigma_1^2}}}\right)+Q\!\left(\frac{2}{\sigma_1}\right)Q\!\left(\frac{-3+\frac{\sigma_1^2}{\sigma_2^2}}{\sigma_1\sqrt{1+\frac{\sigma_1^2}{\sigma_2^2}}}\right),\end{aligned} \tag{4.5}$$

where $Q(\cdot)$ is the Q-function [29].

Using the channel inversion precoder and likelihood detectors [29], the exact BERs for a given channel realization are derived at D_1 as $\mathbb{P}^{\mathrm{S}_1}_{\mathrm{D}_1} \triangleq \mathbb{P}\left(\widehat{x}_1 \neq x_1\right) = Q\left(1/\sigma_{\mathrm{S}_1,\mathrm{D}_1}\right)$ and $\mathbb{P}^{\mathrm{r}}_{\mathrm{D}_1} \triangleq \mathbb{P}\left(\widehat{x}_{\oplus,\mathrm{D}_1} \neq \widehat{x}_{\oplus,\mathrm{r}}\right) = Q\left(1/\sigma_{r,\mathrm{D}_1}\right)$.

Now, $\mathbb{P}_{\mathrm{D}_1}$ is derived as:

$$\begin{aligned}\mathbb{P}_{\mathrm{D}_1} &= \mathbb{P}^{\mathrm{S}_1}_{\mathrm{D}_1}\left(1-\mathbb{P}^{\mathrm{r}}_{\mathrm{D}_1}\right)\left(1-\mathbb{P}^{\mathrm{r}}_{\oplus}\right)+\mathbb{P}^{\mathrm{S}_1}_{\mathrm{D}_1}\mathbb{P}^{\mathrm{r}}_{\mathrm{D}_1}\mathbb{P}^{\mathrm{r}}_{\oplus}\\ &\quad +\left(1-\mathbb{P}^{\mathrm{S}_1}_{\mathrm{D}_1}\right)\mathbb{P}^{\mathrm{r}}_{\mathrm{D}_1}\left(1-\mathbb{P}^{\mathrm{r}}_{\oplus}\right)+\left(1-\mathbb{P}^{\mathrm{S}_1}_{\mathrm{D}_1}\right)\left(1-\mathbb{P}^{\mathrm{r}}_{\mathrm{D}_1}\right)\mathbb{P}^{\mathrm{r}}_{\oplus}.\end{aligned} \tag{4.6}$$

Note that the event $(\widehat{x}_2 \neq x_2)$ at D_1 occurs when the number of links with error is odd. For example, $\mathbb{P}^{\mathrm{S}_1}_{\mathrm{D}_1}\left(1-\mathbb{P}^{\mathrm{r}}_{\mathrm{D}_1}\right)\left(1-\mathbb{P}^{\mathrm{r}}_{\oplus}\right)$ considers that the estimated value of x_1 at D_1 is wrong while $\widehat{x}_{\oplus,\mathrm{r}}$ and $\widehat{x}_{\oplus,\mathrm{D}_1}$ are correct.

4.3 General Sum-difference Matrix

In chapter 2, to show the fundamental idea of PNC, the assumptions are that the relay node has two antennas and each source node has one antenna. Therefore, the size of the sum-difference matrix $\mathbf{D}$ in (2.3) is two-by-two. Such a two-by-two matrix $\mathbf{D}$ will still be workable if the relay has more than two antennas, i.e., $N_{\mathrm{r}} > 2$. Let us consider a more general scenario where N_{sa} is the number of antennas at each source node and $N_{\mathrm{r}} > N_{\mathrm{sa}}$. In this scenario, the size of the sum-difference matrix should be $2N_{\mathrm{sa}}$-by-$2N_{\mathrm{sa}}$, and it could be written

$$\mathbf{D}_{2N_{\mathrm{sa}}\times 2N_{\mathrm{sa}}} = \begin{bmatrix} \mathbf{D} & 0 & 0 & \cdots & 0 \\ 0 & \mathbf{D} & 0 & \cdots & 0 \\ 0 & 0 & \mathbf{D} & \cdots & 0 \\ \vdots & \vdots & \vdots & \ddots & \vdots \\ 0 & 0 & 0 & 0 & \mathbf{D} \end{bmatrix}, \tag{4.7}$$

where $\mathbf{D}$ is the sum-difference matrix shown in (2.3). The important idea behind PNC is to obtain a sum-difference matrix that satisfies the conditions below:

- there is a little information loss when the received signal is linearly transformed to the mixed form;
- there is a little information loss when the network-coding form is obtained from a mix of original signal $\mathbf{x}$ and the sum-difference matrix.

Chapter 5

Results and Evaluation

In this Chapter, we demonstrate the advantages of using IRS and PNC in terms of the BER. The coefficients of the channels are generated as standard complex Gaussian random variables. The SNR is defined as SNR $\triangleq P/\sigma^2$. In all figures, solid and dashed lines represent theoretical and Monte-Carlo simulation results averaged over many realizations of the channels, respectively.

5.1 Evaluation at the Relay

To evaluate the impact of the IRS phase design, the BER at the relay, $\mathbb{P}^{\mathrm{r}}_{\oplus}$, versus SNR is depicted in Fig. 5.1 for two network coding schemes (PNC and NNC), two architectures (with and without IRS) and for various phase designs, i.e., *i) optimal:* the phases are designed according to the proposed scheme in Chapter 3; *ii) quantized:* the optimal phases are quantized to two levels (0 or π); *iii) random:* the phases are selected uniformly at random from 0 to $2\,\pi$. As can be noticed from Fig. 5.1, implementing just PNC without IRS offers a little SNR gain around 1 dB over traditional NNC scheme for a target BER of 10^{-3}. Adding IRS and optimizing its phases can significantly decrease the BER. According to Fig. 5.1, PNC approach with optimal phases has SNR gain around 28 dB over traditional NNC scheme for a target BER of 10^{-3}. Moreover, the SNR gains compared to quantized phases and random phases are about 3.5 dB and 17 dB, respectively. The resulting matrix from the multiplication of matrices $\mathbf{G}$ and $\widetilde{\mathbf{H}}$ is close to the identity matrix at SNRs higher than -20 dB,

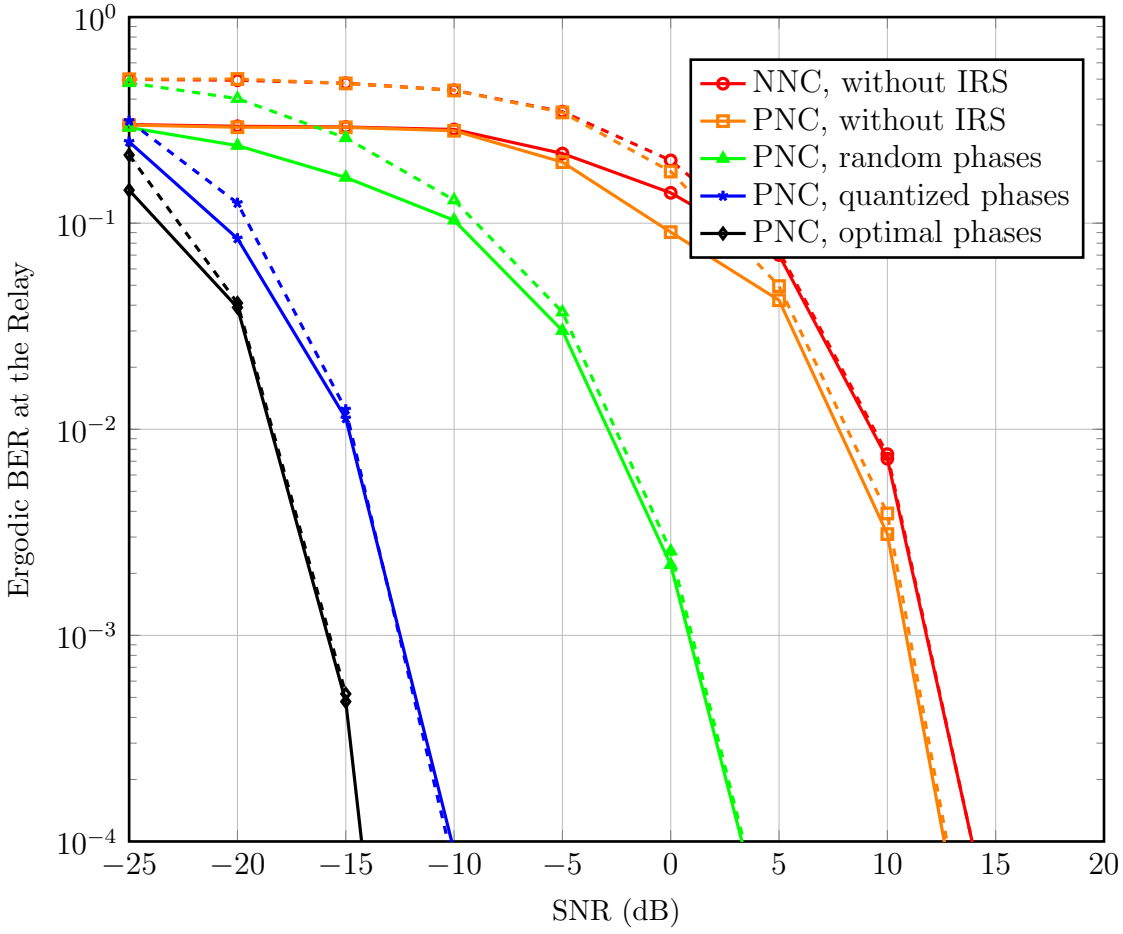

Figure 5.1: Ergodic BER at the relay, $\mathbb{P}^{\mathrm{r}}_{\oplus}$, as a function of SNR, for $M = 32$.

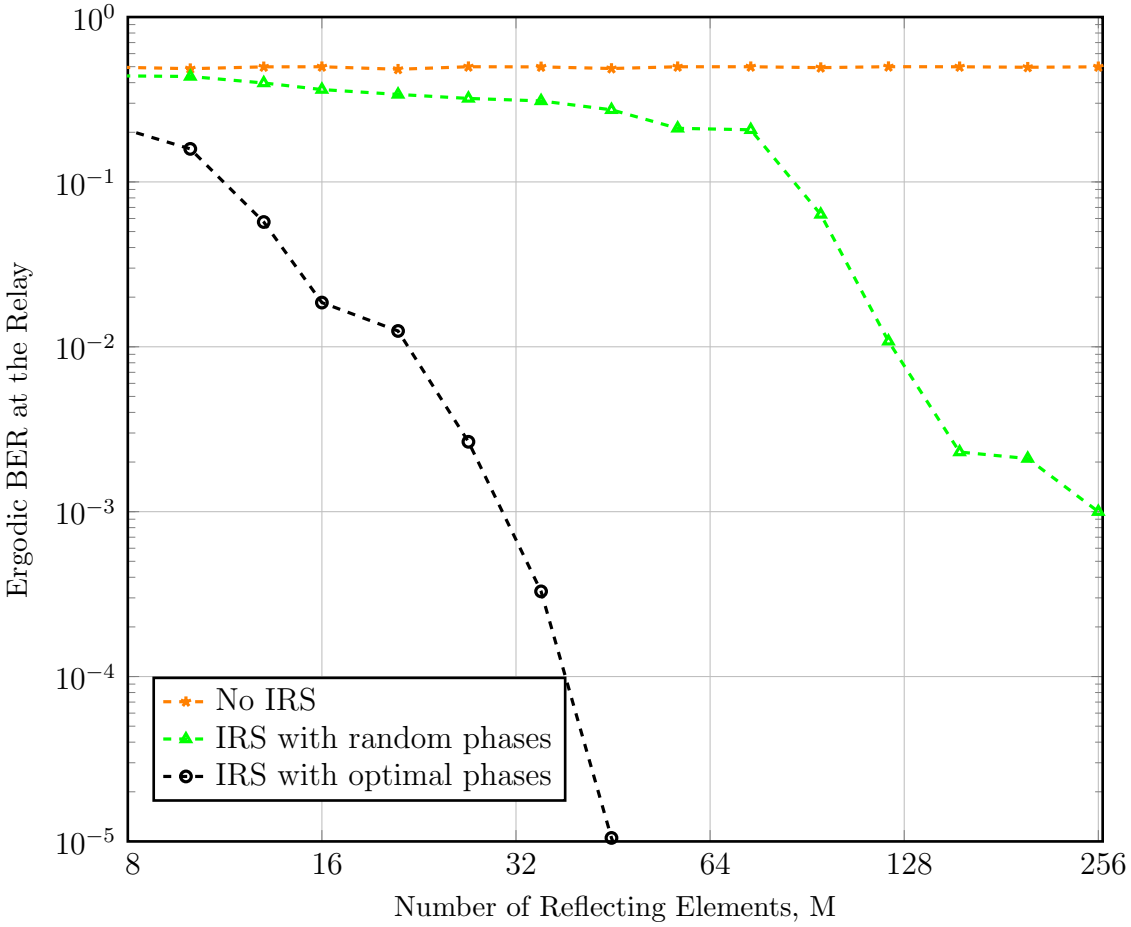

Figure 5.2: Ergodic BER at the relay, $\mathbb{P}^{\mathrm{r}}_{\oplus}$, as a function of M at SNR $= -15$ dB.

-15 dB, -5 dB, 5 dB and 5 dB for the PNC approach with optimal phases, quantized phases, random phases, without IRS and traditional NNC approach without IRS, respectively. Therefore, you can notice that, in this regions, the Monte-Carlo simulations start to coincide with the theoretical results.

The impact of the number of reflecting elements at IRS on the BER at the relay is shown in Fig. 5.2. Two phase profiles are considered (optimal and random) along with the case without IRS. For random phases, $\mathbb{P}_{\mathrm{D}_1}$ decreases slowly, while the proposed phase design allows the BER to decrease with M rapidly. As can be seen from Fig. 5.2, the BER at the relay in the presence of a 32-element IRS with random phases is slightly less than that without an IRS while, for a 32-element IRS with optimal phases, the BER at the relay is three orders of magnitudes less than that without an IRS.

In Fig. 5.3, the ergodic MSE is plotted versus SNR at the relay. As can be noticed from Fig. 5.3, without IRS, the gap between traditional NNC and proposed PNC in terms of MSE calculated at the relay is noticeable at low SNR and high SNR regions. MSE derived in (3.2) can be further reduced with the help of IRS. According to Fig. 5.3, the gap between PNC without IRS and PNC with optimal phases of IRS in terms of MSE is significant and increases with SNR. Therefore, Fig. 5.3 shows important information that using PNC in IRS-assisted environment offers noticeable gain.

5.2 Evaluation at the Destination

In Fig. 5.4, we assess the impact of two network coding schemes (PNC and NNC) and two architectures (with and without IRS) on the BER at the destination node, D_1. We can see that the proposed scheme, i.e., PNC combined with IRS, outperforms the schemes that consider PNC and NNC without IRS. BER at D_1, $\mathbb{P}_{\mathrm{D}_1} = 10^{-3}$, is achieved at SNR = 12.8 dB and SNR = 12.3 dB for the case when we use traditional NNC and proposed PNC approaches without IRS, respectively. The PNC

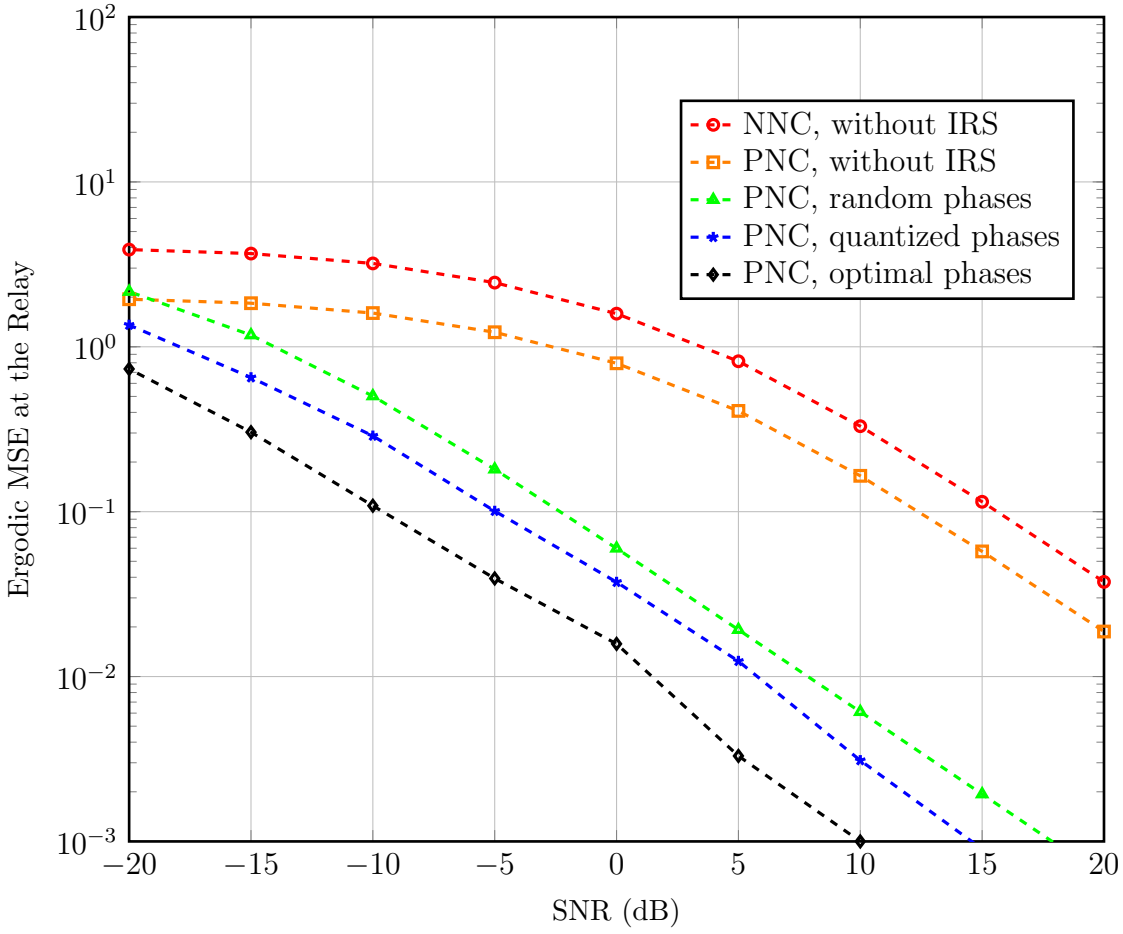

Figure 5.3: Ergodic MSE at the relay as a function of SNR, for $M = 32$.

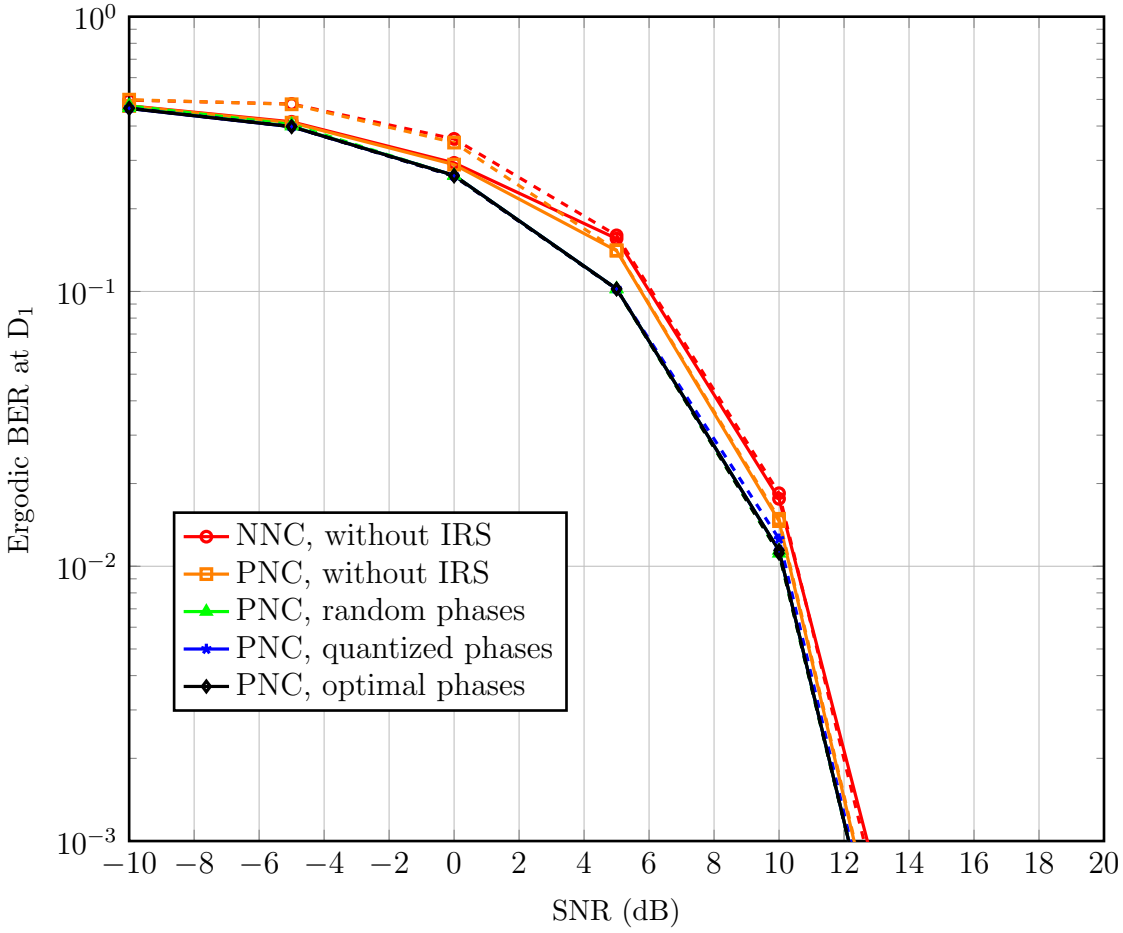

Figure 5.4: Ergodic BER at D_1, $\mathbb{P}_{D_1}$, as a function of SNR, for $M = 32$.

with random, quantized and optimal phases have $\mathbb{P}_{D_1} = 10^{-3}$ at SNR = 12.1 dB, SNR = 14.08 dB and SNR = 12.05 dB, respectively. Hence, for target $\mathbb{P}_{D_1} = 10^{-3}$, the SNR gain of proposed scheme compared to traditional NNC without IRS is around SNR = 0.75 dB. Surprisingly, in contrast to the error experienced at the relay in Fig. 5.1, the gap between the PNC approaches with different IRS designs is negligible. This is attributed to the fact that the BER for the direct link between S_1 and D_1, $\mathbb{P}_{D_1}^{S_1}$, dominates the effect of $\mathbb{P}_{\oplus}^{r}$, while computing the BER at the relay in (4.5). Therefore, future works can consider adding two IRSs to enhance the direct links from the sources to destinations, i.e., $S_1 - D_1$ and $S_2 - D_2$.

Chapter 6

Concluding Remarks

6.1 Summary

We proposed an IRS-aided PNC to improve the wireless network throughput and BER performance. The main contribution is our novel design with IRS that estimates the XOR value of two symbols over-the-air with optimal IRS phases to minimize the estimation error. Also, we derived analytical expressions for the BER. The numerical results show that jointly optimizing the IRS phases and beamforming matrix at the relay offers better performance in terms of the BER. For instance, the BER at the relay in a 32-element IRS-assisted environment is three orders of magnitudes less than that without IRSs. For a target BER of 10^{-3}, we can achieve around 28 dB and 0.75 dB performance gains in SNR at the relay and destinations compared to naive network coding without IRS, respectively.

6.2 Future Research Direction

As future research directions, our proposed approach can be implemented and analyzed on more complicated network structures such as cockroach network, etc. However, for more complicated network structures, the network coding function will also be more complicated than just computing the XOR of two signals. In addition, multiple IRSs can be deployed in more complicated network structures to enhance the communication performance of the networks. However, jointly-optimizing them is a computationally formidable challenge. Hence, to perform efficient deployment de-

sign of IRSs, new mathematical tools such as machine learning [30] and stochastic geometry [31–33] need to be considered.

REFERENCES

[1] J. Sykora and A. Burr, *Wireless Physical Layer Network Coding*. Cambridge University Press, 2018.

[2] K. W. Choi, A. A. Aziz, D. Setiawan, N. M. Tran, L. Ginting, and D. I. Kim, "Distributed wireless power transfer system for internet of things devices," *IEEE Internet of Things Journal*, vol. 5, no. 4, pp. 2657–2671, 2018.

[3] J. Guo, S. Durrani, X. Zhou, and H. Yanikomeroglu, "Massive machine type communication with data aggregation and resource scheduling," *IEEE Trans. Commun.*, vol. 65, no. 9, pp. 4012–4026, 2017.

[4] S. Katti, H. Rahul, W. Hu, D. Katabi, M. Médard, and J. Crowcroft, "XORs in the air: practical wireless network coding," *IEEE/ACM Trans. Netw.*, vol. 16, no. 3, pp. 497–510, 2008.

[5] O. Kosut, L. Tong, and D. Tse, "Nonlinear network coding is necessary to combat general byzantine attacks," in *Proc. 2009 47th Annu. Allerton Conf. Commun. Control Comput.*, 2009, pp. 593–599.

[6] S. Zhang and S. C. Liew, "Physical layer network coding with multiple antennas," in *2010 IEEE Wireless Commun. Netw. Conf.*, 2010.

[7] N. Lee, J.-B. Lim, and J. Chun, "Degrees of freedom of the MIMO Y channel: Signal space alignment for network coding," *IEEE Trans. Inf. Theory*, vol. 56, no. 7, pp. 3332–3342, 2010.

[8] Q. Wu and R. Zhang, "Weighted sum power maximization for intelligent reflecting surface aided swipt," *IEEE Wireless Communications Letters*, vol. 9, no. 5, pp. 586–590, 2019.

[9] T. Jiang, H. V. Cheng, and W. Yu, "Learning to beamform for intelligent reflecting surface with implicit channel estimate," *arXiv preprint arXiv:2009.14404*, 2020.

[10] Z. Huang, B. Zheng, and R. Zhang, "Transforming fading channel from fast to slow: Irs-assisted high-mobility communication," *arXiv preprint arXiv:2011.03147*, 2020.

[11] M. Di Renzo *et al.*, "Smart radio environments empowered by reconfigurable AI meta-surfaces: An idea whose time has come," *EURASIP J. Wireless Commun. Netw.*, vol. 2019, no. 1, pp. 1–20, 2019.

[12] Q. Wu and R. Zhang, "Intelligent reflecting surface enhanced wireless network: Joint active and passive beamforming design," in *IEEE Global Communications Conference (GLOBECOM)*. IEEE, 2018, pp. 1–6.

[13] Q. Wu, S. Zhang, B. Zheng, C. You, and R. Zhang, "Intelligent reflecting surface aided wireless communications: A tutorial," *IEEE Trans. Commun.*, 2021, to appear.

[14] D. Yu, S.-H. Park, O. Simeone, and S. S. Shitz, "Optimizing over-the-air computation in IRS-aided C-RAN systems," in *Proc. 2020 IEEE 21st Int. Workshop Signal Process. Advances Wireless Commun. (SPAWC)*, May 2020.

[15] Q. Wu and R. Zhang, "Towards smart and reconfigurable environment: Intelligent reflecting surface aided wireless network," *IEEE Commun. Mag.*, vol. 58, no. 1, pp. 106–112, Jan. 2020.

[16] M. A. Kishk and M.-S. Alouini, "Exploiting randomly-located blockages for large-scale deployment of intelligent surfaces," *IEEE J. Sel. Areas Commun.*, Apr. 2021.

[17] C. Huang, A. Zappone, G. C. Alexandropoulos, M. Debbah, and C. Yuen, "Reconfigurable intelligent surfaces for energy efficiency in wireless communication," *IEEE Trans. Wireless Commun.*, vol. 18, no. 8, pp. 4157–4170, Aug. 2019.

[18] H. Ibraiwish, A. Elzanaty, Y. H. Al-Badarneh, and M.-S. Alouini, "EMF-aware cellular networks in RIS-assisted environments," Jan. 2021. [Online]. Available: http://hdl.handle.net/10754/666963

[19] L. Chiaraviglio, A. Elzanaty, and M.-S. Alouini, "Health risks associated with 5G exposure: A view from the communications engineering perspective," *arXiv preprint arXiv:2006.00944*, 2020.

[20] A. Elzanaty, A. Guerra, F. Guidi, and M.-S. Alouini, "Reconfigurable intelligent surfaces for localization: Position and orientation error bounds," arXiv:2009.02818 [cs.IT]., Sep. 2020.

[21] W. Fang, M. Fu, K. Wang, Y. Shi, and Y. Zhou, "Stochastic beamforming for reconfigurable intelligent surface aided over-the-air computation," arXiv:2005.10625 [cs.IT]., May 2020.

[22] T. Jiang and Y. Shi, "Over-the-air computation via intelligent reflecting surfaces," in *Proc. 2019 IEEE Global Commun. Conf. (GLOBECOM)*, Dec. 2019.

[23] R. Ahlswede, N. Cai, S.-Y. Li, and R. W. Yeung, "Network information flow," *IEEE Trans. Inf. Theory*, vol. 46, no. 4, pp. 1204–1216, 2000.

[24] M. P. Wilson, K. Narayanan, H. D. Pfister, and A. Sprintson, "Joint physical layer coding and network coding for bidirectional relaying," *IEEE Trans. Inf. Theory*, vol. 56, no. 11, pp. 5641–5654, Nov. 2010.

[25] Z.-Q. Luo, W.-K. Ma, A. M.-C. So, Y. Ye, and S. Zhang, "Semidefinite relaxation of quadratic optimization problems," *IEEE Signal Process. Mag.*, vol. 27, no. 3, pp. 20–34, May 2010.

[26] Q. Wu and R. Zhang, "Intelligent reflecting surface enhanced wireless network via joint active and passive beamforming," *IEEE Transactions on Wireless Communications*, vol. 18, no. 11, pp. 5394–5409, 2019.

[27] M. Tao, E. Chen, H. Zhou, and W. Yu, "Content-centric sparse multicast beamforming for cache-enabled cloud RAN," *IEEE Trans. Wireless Commun.*, vol. 15, no. 9, pp. 6118–6131, Sep. 2016.

[28] G. C. Calafiore, S. Gaubert, and C. Possieri, "A universal approximation result for difference of log-sum-exp neural networks," *IEEE Trans. Neural Netw. Learning Syst.*, vol. 31, no. 12, pp. 5603–5612, Dec. 2020.

[29] J. G. Proakis and M. Salehi, *Digital Communications*. McGraw-Hill., 2008.

[30] L. Wei, C. Huang, G. C. Alexandropoulos, and C. Yuen, "Parallel factor decomposition channel estimation in RIS-assisted multi-user MISO communication," in *2020 IEEE 11th Sensor Array and Multichannel Signal Processing Workshop (SAM)*. IEEE, 2020, pp. 1–5.

[31] S. Hu, F. Rusek, and O. Edfors, "Beyond massive MIMO: The potential of data transmission with large intelligent surfaces," *IEEE Trans. Signal Process.*, vol. 66, no. 10, pp. 2746–2758, 2018.

[32] M. Hua, Q. Wu, D. W. K. Ng, J. Zhao, and L. Yang, "Intelligent reflecting surface-aided joint processing coordinated multipoint transmission," *IEEE Transactions on Communications*, 2020.

[33] H. Liu, X. Yuan, and Y.-J. A. Zhang, "Matrix-calibration-based cascaded channel estimation for reconfigurable intelligent surface assisted multiuser MIMO," *IEEE Journal on Selected Areas in Communications*, vol. 38, no. 11, pp. 2621–2636, 2020.